

# ON THE MESO-MECHANICAL MODELING METHOD FOR TEXTILE COMPOSITES

Chao Zhang<sup>1</sup> and Yulong Li<sup>2</sup>

<sup>1</sup> Department of Aeronautical Structure Engineering, Northwestern Polytechnical University, Xi'an Shaanxi, China 710072,

Email: [chaozhang@nwpu.edu.cn](mailto:chaozhang@nwpu.edu.cn), Website: <http://teacher.nwpu.edu.cn/chaozhang.html>.

<sup>2</sup> Department of Aeronautical Structure Engineering, Northwestern Polytechnical University, Xi'an Shaanxi, China 710072,

Email: [liyulong@nwpu.edu.cn](mailto:liyulong@nwpu.edu.cn), Website: <http://teacher.nwpu.edu.cn/liyulong.html>.

**Keywords:** Meso-mechanical model, Finite element, Triaxially braided composites, Progressive damage simulation, Periodic boundary conditions

## ABSTRACT

Textile composites are well known for their excellent through thickness properties and impact resistance. The braided architecture produces significant difficulty on the computational simulation, especially on the modelling of the progressive damage behaviour. In this work, we present a conclusive study on the methodology of meso-mechanical model for textile composites based on previous series of studies. We introduce first the procedures for generating a representative unit cell model and its finite element mesh of a triaxially braided composite, based on the composite fiber volume ratio, specimen thickness and microscopic image analysis. Through a series of numerical studies, we highlight the importance of imposing proper boundary conditions when correlating with experimental results. The results suggest that a translational symmetrical boundary condition with sufficient number of unit cells for straight-sided coupon specimens is efficient and provides excellent accuracy on failure simulation. We also propose the potential application of meso-mechanical model on visual testing, and present preliminary results of failure modelling for notched and tube tensile specimens using meso-mechanical models. The results of this work intends to provide a benchmark example on conducting meso-mechanical modelling of textile composites.

## 1 INTRODUCTION

Fiber reinforced composite materials are being widely used in various manufacturing such as aerospace, automotive, marine and sporting equipment due to their outstanding physical, mechanical and thermal properties. In recent years, textile composites have emerged as leading contenders in industrial sectors because its more excellent properties than traditional laminated structures in terms of damage tolerance and energy absorption [1], so engine manufactures try to fabricate new engine fan cases by employing textile composites, to contain the blade and fragments during engine blade out event, and bird strike also need to be considered.

Meso-scale modeling approach is a widely used methodology in the analysis of textile composites due to their excellent ability to simulate local damage processes. Ivanov et al. [2] studied the damage and failure behavior of triaxially braided carbon/epoxy composites under tension using a meso-scale finite element model. Progressive damage and stiffness degradation was modeled using the degradation scheme of Murakami–Ohno and the damage evolution law of Ladeveze, applied to the average stress state of the yarns. Schultz and Garnich [3] predicted the initial matrix failure and overall composite failure under multi-axial loading by using a combination of a meso-scale finite element model and the multi-continuum modeling method. The model's predictions were in good agreement with experimental data and the results that would be expected by physical intuition. The main features of a meso-scale finite element model are a realistic mesh of the fiber bundle geometry, homogenized local properties of the impregnated fiber tows accounting for the realistic local fiber volume ratio and orientation, and an accurate definition of boundary conditions [4]. In our previous work, a series of studies have been conducted to study the progressive failure behaviour of a triaxially braided

composite using meso-mechanical models, where a few critical issues have been identified for the meso-mechanical modelling approach [5-8]. For example, the finite element model geometry and mesh should include key features of the actual architecture, such as unit cell size, local fiber volume ratio in each fiber bundle and fiber bundle dimensions. These geometric parameters have a significant effect on the modeling results. Due to differences in the manufacturing process, the values of these geometric parameters vary significantly for different material systems. So, when correlating with experimental results, the finite element model should first ensure the critical geometry parameters are incorporated correctly. And a general framework for generating the finite element mesh could greatly facilitate the modelling efficiency.

In the present paper, we introduce briefly the procedure of generating a meso-mechanical model and discuss mainly the effect of boundary condition and size on the numerical results. We highlight the advantages of meso-mechanical model on predicting the progressive damage behaviour of a two-dimensional triaxially braided composite, and apply the developed model to evaluate the capability of different types of test specimens on obtaining more representative mechanical properties.

## **2 DEVELOPMENT OF A MESO-MECHANICAL MODEL**

### **2.1 Material**

The  $0^\circ/\pm 60^\circ$  braided composite studied in the present study is fabricated with 24K T700s axial tows and 12K T700s bias tows, as shown in Figure 1(a). The composite panels were processed through resin transfer molding. The properties of each component can be found in Ref [9]. The sample considered in the present study is a single-layer panel with a fiber volume ratio of 0.48. The panel was manufactured into straight-sided coupons that were 35.56 mm wide by 304.8 mm long (1.4 in. wide by 12 in. long).

### **2.2 Geometrical modeling**

To model the realistic geometrical feature, an image analysis is conducted on the microscopic cross-section image to extract the average geometry parameters of fiber bundles. Based on the obtained geometric parameters, a finite element model was generated. First, the geometric model for the braided composite (shown in Figure 1(b)) was constructed using the TEXGEN software (Version 3.5.2) TexGen 3.5.2 by inputting the unit cell and fiber bundle dimensions. The fiber bundles are all assumed to have an elliptical cross sectional shape based on the cross section area and width. The meso-scale finite element mesh for a unit cell shown in Figure 2(a) (matrix elements are hidden) and (b) was then generated automatically through TEX- GEN. There are 13520 elements for the unit cell, 10 elements through the thickness, 26 elements in the axial direction and 52 elements along the transverse direction. In the figure, the matrix elements are colored gray, the axial fiber bundle elements are colored dark blue, the  $+60^\circ$  bias fiber bundle elements are colored light blue, and the  $60^\circ$  bias fiber bundle elements are colored green. Eight-node hexahedron elements were used for the finite element mesh in the current study. Although coarse edges were observed for the bias fiber bundles, they were found to have no significant influence on the analysis, as will be shown in a later section of the current paper. Also, as seen in Figure 2(b), the model of the axial fiber bundles avoids sharp edges, which were shown in the previous work to result in highly distorted elements and promote the prediction of significant local damage.

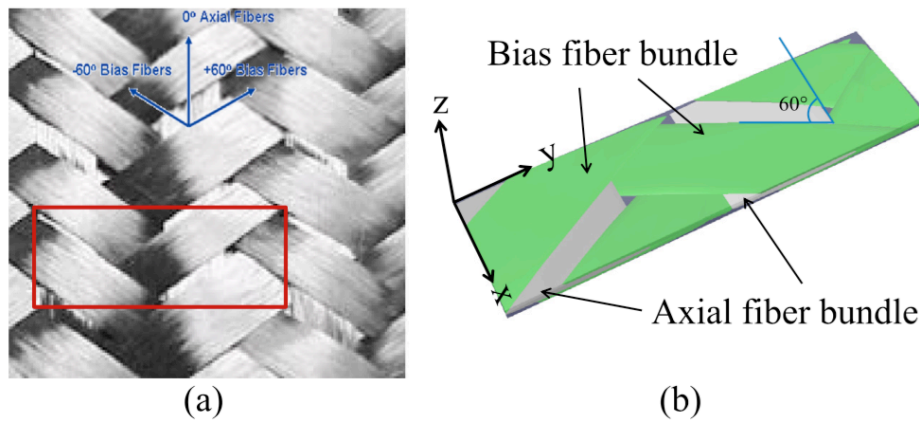


Figure 1: (a)  $^{\circ}/\pm 60^{\circ}$  triaxial braided carbon fabric architecture and (b) model representation. [5]

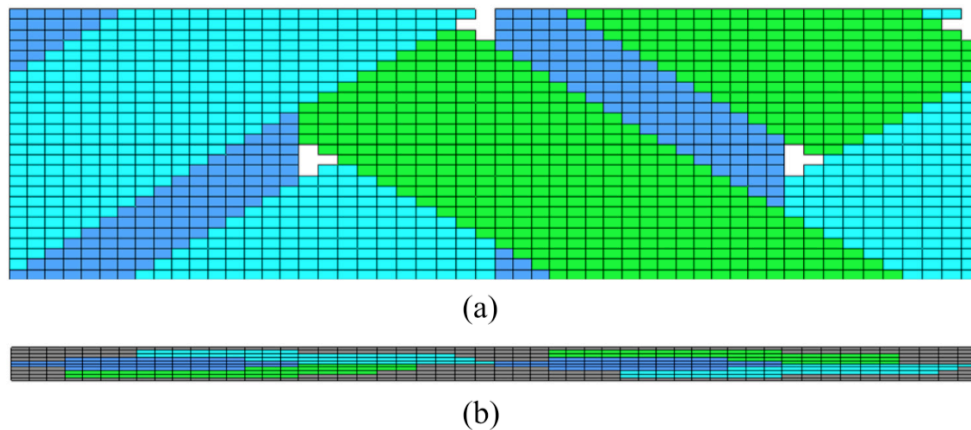


Figure 2: (a) Top view of the finite element mesh of a braided composite unit cell model (matrix is not shown for clarity) and (b) side view of the braided composite finite element model. [5]

### 2.3 Model Correlation

The fiber bundles are modeled as transverse isotropic unidirectional lamina. The matrix is generally modeled as plastic materials, and can be simplified as bilinear elastic-plastic material considering the small failure strain of composites. The damage-evolution model of fiber bundles is based on fracture energy dissipated during the damage process, characteristic length of element and equivalent displacement. Hashin-type failure criteria are employed to determine damage initiation. A cohesive law is introduced to simulate interface failure, near elastic before satisfying one of the damage modes. In the tensile fiber failure criteria [5], a coefficient  $\alpha$  with a value between 0 and 1 is employed to determine the contribution of shear stress to the initiation of fiber tensile failure. Unlike traditional laminated composites, under axial or transverse tensile loading conditions braided composites are known to have obvious free-edge effect and subject to relatively large in-plane shear stresses due to the complex fiber architecture. Properly accounting for the effects of shear stresses on the fiber tensile mode failure of the fiber tows is necessary for appropriately modeling the global composite behavior.

Figure 3 shows the comparison between experimental measured stress-strain curves and numerical simulation curves with different shear weighting factor values, in the case of using a two-dimensional Hashin failure criteria to model the failure of fiber bundle. In this study, the coefficient  $\alpha$  was determined based on correlation of numerical and experimental results which will be presented later in this paper. As we can see from Figure 3, all the numerical curves match well with each other in modulus, but show different ultimate strengths, especially under the transverse tension loading condition. This indicates that coefficient  $\alpha$  has an obvious impact on the global stress-strain response

and mainly on the failure prediction. The experiment ultimate strength is highlighted using a triangle symbol in the plot and is very close to the predicted curve when  $\alpha = 0.4$  for axial fiber bundle and  $\alpha = 0.8$  for transverse fiber bundles. In a different study where a three-dimensional failure criteria is used [10],  $\alpha$  is correlated to be 0.06 for both axial and bias fiber bundles.

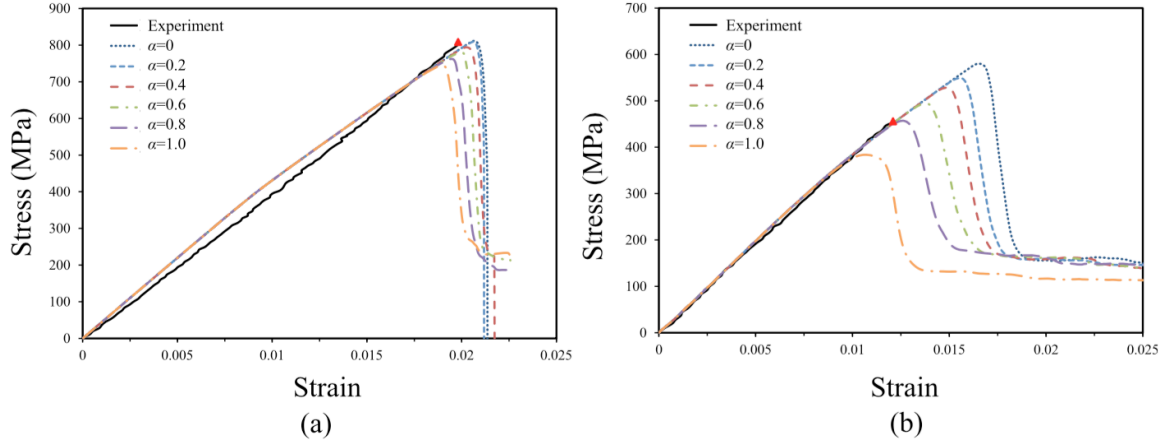


Figure 3: Global stress–strain curves of axial tension (a) and transverse tension (b) models with different shear weighting factor values. [5]

### 3 EFFECT OF BOUNDARY CONDITION

A primary advantage of using a meso-scale finite element approach for analyzing the response of composites is in predicting full field deformation and local strain distribution. One specific failure behavior of triaxially braided composite is the presence of free-edge effect during tension, especially under transverse tension. The free-edge effect of triaxial braided composite was identified by Kohlman et al. [11] and found to act in the form of free-edge warping. The free-edge warping is formed due to the termination of fiber tows at the free edges, resulting a discontinuous of load transferring and further a out-of-plane shear deformation. Thus, it is necessary to examine the ability of meso-scale model in capturing this phenomenon.

Proper boundary conditions should be applied to the unit cell models during fundamental analyses meant to check the correlation with experimental responses. Quek et al. [12] and Song et al. [13] utilized a finite element based meso-mechanical model for studying the compression response of a triaxially braided textile composite and proposed symmetrical boundary is sufficiently accurate. In Quek's, Song's and Li's work [12-14], symmetric loadings and boundary conditions were considered. Lomov et al. [4] discussed the stages of a meso-scale finite element analysis and proposed the necessary of imposing periodic boundary conditions. In this work, models with periodical boundary condition (Per BC) and symmetrical loading boundary condition (Sym BC) were both studied to examine the role of boundary conditions in free-edge effect simulation.

As shown in Figure 4, the two models with Per BC and Sym BC show different out-of-plane deformations, and transverse tension case present more serious edge warping with much higher warping magnitude. Compared with the experimental results (Ref to [11]), the Per BC model predicts the free-edge effect excellently, especially in transverse tension, capturing not only the anti-symmetrical free-edge warping behavior but also the warping magnitude and size of propagation area. While the Sym BC model presents more serious edge warping under transverse tension due to the lack of continuity along the loading direction. For the same reason, the Sym BC model shows warping along the loading edges under axial tension condition, due to the bias fiber tow termination at the loading edges. When periodical boundary condition applied, the two loading edges are assumed to be continuous which avoids bias fiber tow termination along the loading direction, and concave/convex curvatures are produced periodically along the free-edges capturing the experimental phenomenon in some extent. Through the numerical simulation, we can found that the bias fiber tow termination/continuity plays a great role in producing the free-edge effect. It is also concluded by

Kueh [15] that bias fiber tow termination causes the size-dependent elastic properties of triaxial braided composite, which is further proved experimentally and numerically by Zhang et al. [8] and will be introduced in the next section.

Overall, the developed meso-scale Per BC model predicts the free-edge effect under both axial and transverse tension case in a very good manner. On the other hand, the Sym BC model although is able to match the global stress-strain responses, shows limitations in modeling the inherent damage behavior and failure progression. Thus, it is important to impose proper boundary condition when correlating with experimental results.

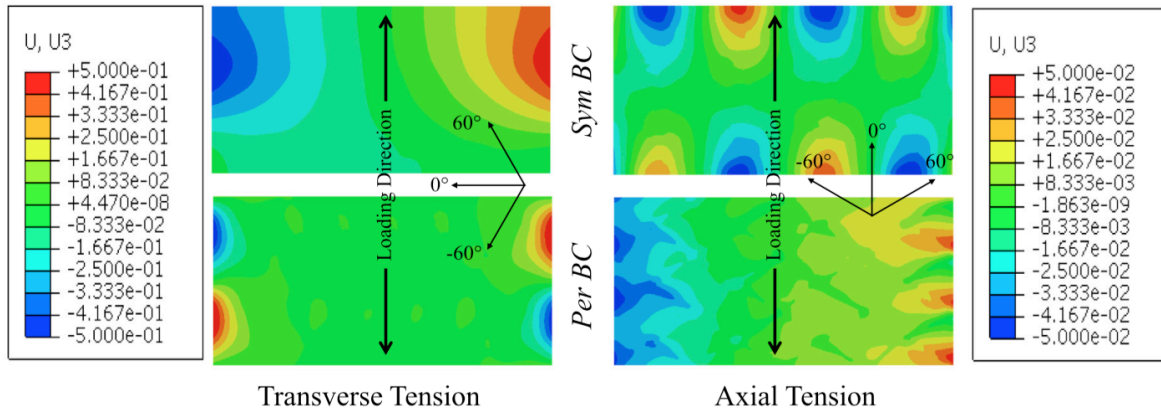


Figure 4: Surface out-of-plane deformation contours of Per BC and Sym BC model under axial and transverse tension. [5]

#### 4 SIZE EFFECT AND FREE-EDGE EFFECT

Another important issue for textile composites is their size dependency of mechanical properties. Figure 5(a) shows the experimental stress–strain curves of the transverse tension coupon specimens. As shown in this figure, the stress–strain curves display an obvious size-dependency, as increasing the specimen width results in a higher effective transverse tension modulus and ultimate transverse tension failure strength. As shown in Figure 5(b), the numerically predicted moduli match well with the experimental results, indicating the capability of this meso-scale finite element model to simulate the elastic response. In terms of size-dependency, both numerical and experimental results display an increasing transverse modulus value with an increase of specimen width. The dependence of the transverse modulus on the specimen width is believed to be related to the edge-effect-initiated free-edge warping.

Figure 6(a) presents the DIC images of out-of-plane displacement contours for each of the varied width specimens. Periodic warping behavior is observed along the free edges for all specimens at locations where the bias fiber tows intersect. It is also found that the warping shows an interaction and anti-symmetrical distribution of positive motion and negative motion. In the transverse tension case, loads are handled by bias fiber tows as the axial fiber tows are now perpendicular to the loading direction. Since most of the bias fiber tows terminate at the free edge, the load is not able to transfer from one boundary end to the next and can only be transmitted between the tows through interlocking and scissoring actions. Figure 6(b) shows the warping location and direction of a transverse tension specimen. An ellipsis shown in red or blue indicates the specific location of positive and negative out-of-plane displacement. Due to the cutting of the specimen, the top and bottom free edges line up with each other, i.e. the specimen has a continuous layout, and the two free edges match if the specimen is duplicated and translated. For the analyzed location on the top free edge, since the undulation tendency of the related fiber tows are going up out of the plane along the loading direction, the warping tendency of this area will be going out of plane; conversely, for the corresponding location at the bottom free edge, the fiber tows tend to undulate down along the loading direction, resulting in the opposite warping behavior. The alternate positive and negative warping along the free edges then results in the anti-symmetric displacement distribution.

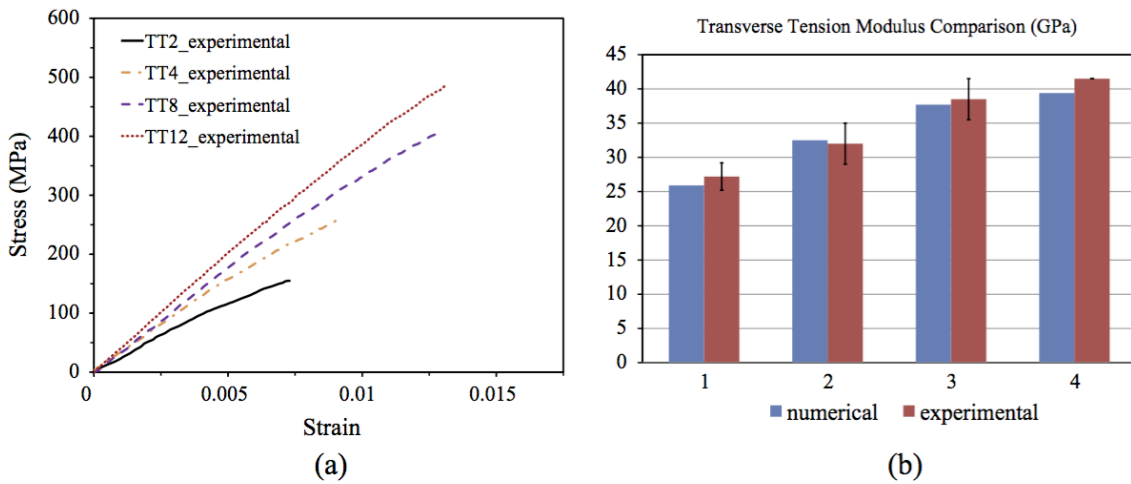


Figure 5: (a) Global stress strain responses of transverse tension specimens with different widths and (b) comparison of numerically predicted and experimental measured transverse moduli.[8]

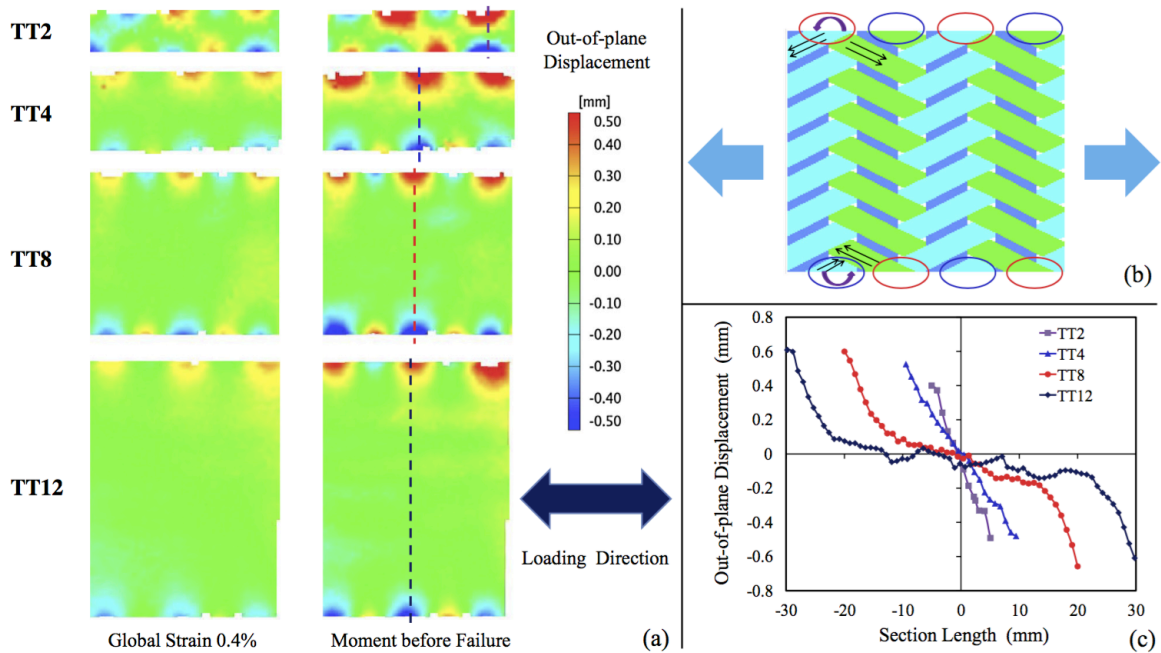


Figure 6: Free-edge warping behavior (a) out-of-plane displacement of varies width specimens; (b) scheme of warping location and direction and (c) section line data of out-of- plane displacement. [8]

Comparing the out-of-plane displacement contours of varied width specimens at the same global strain level, we can also find that the magnitudes of the displacement and warping areas (defined as the area of the specimen that undergoes warping) for all specimens are similar. The proportion of warping area will therefore be smaller in wider specimens, and thus the edge effect should have a smaller effect on the overall effective stiffness, resulting in a relatively larger effective modulus in wider specimens. Figure 6(c) shows the gage section line data (out-of-plane displacement) across the specimen width of each transverse tension specimen. The data indicate that the edge effect (in the form of out-of-plane warping) affects the entire gage section of specimens TT2 and TT4, affects about the first 10 mm (approximately 2-unit-cell widths) of depth into the center from the free edge for specimens TT8 and TT12, and has negligible impacts on the center area of specimens TT8 and TT12. Therefore, we can expect that with the increase of specimen width, the measured modulus value will

continue to increase. However, a large specimen is costly and may introduce more difficulties in tests. For example, the force required to fail the specimen may be above the capability of typical testing machines. Therefore, virtual testing using meso-mechanical model provide a good tool to gain a further understanding of the free-edge effect in this composite material.

## 5 VIRTUAL TESTING USING MESO-MECHANICAL MODEL

A predictable computational model that simulates the tests can provide a detailed expectation of failure modes and offer alternative examination of the potential failure mechanisms of large-scale tests. The developed meso-mechanical finite element model can be applied to evaluate the design of test specimens and to predict effective properties for a multiscale finite element framework for impact simulation. As a demonstration, this paper introduces some preliminary work of using meso-mechanical model to evaluate the notched and tube specimens under tension.

### 5.1 Notched tensile tests

The notched specimen forces a tensile failure for the braided composite and increased measured tensile strength to a reasonable level. Figure 7 shows the comparison of numerical predicted and experimental measured strain contour. The simulation results match the local strain distribution of the axial tension notched specimen in a good manner, capturing the local strain concentration and the damage propagation paths (along the axial and bias direction). And both experimental and numerical results show an anti-symmetrical distribution of shear strain, the origin of which should be the specific braided architecture of this triaxially braided composite. According to the shear strain contour, free-edge effect induced warping behavior is eliminated. However, high shear strain concentration is observed at the notch tips. It is expected that the shear strain concentration will develop into fiber tow transverse failure in tension mode, and ultimately result in fiber tow fracture located at the notch tips.

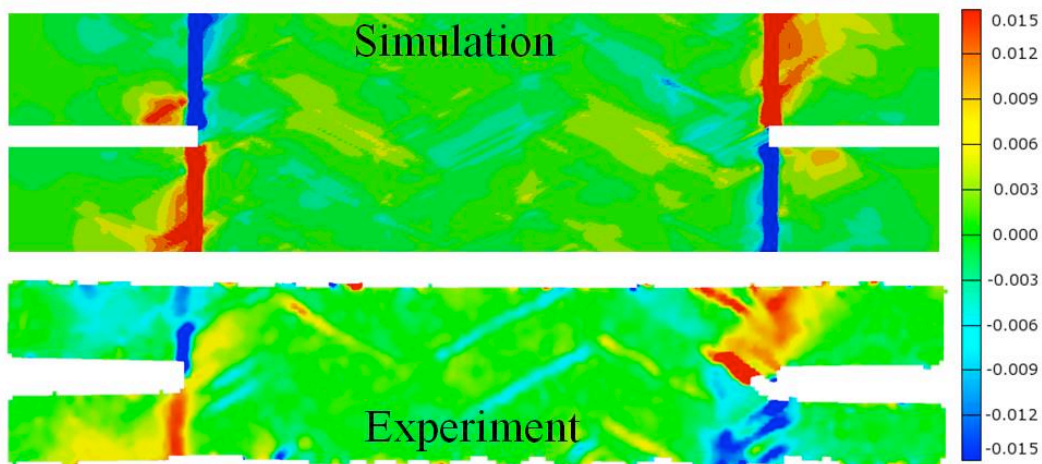


Figure 7: Comparison of numerical and experimental in-plane shear strain contours at a global strain level of 0.5%.

### 5.2 Tube tensile tests

The tube specimen avoids free edges and is supposed to provide properties independent with size. Figure 8 shows the surface shear strain contours of axial and transverse tube specimens at a global strain level of 0.5%. The surface shear strain contours are plotted in a local cylindrical coordinate. As we can see, the shear strain concentrates at the bias fiber tow interaction regions and propagates along the bias fiber tows, similar to the strain distribution of the infinite large straight-sided coupon specimens reported in [5-8]. The magnitude of shear strain at the same global strain level (1.2%) is lower than that of the straight-sided coupon specimen (the maximum shear strain is reported to be

0.015 presented along the free-edge region [11]).

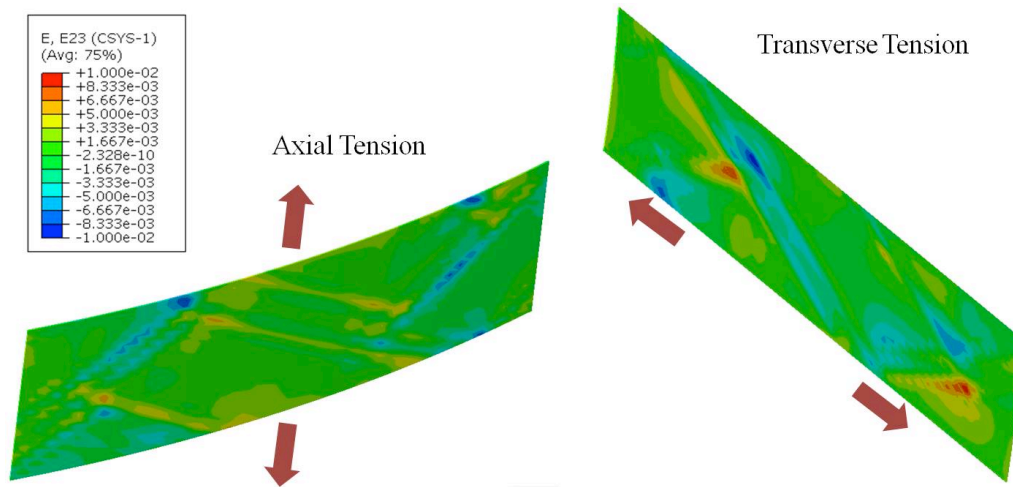


Figure 8: Surface shear strain contours of tube specimens at a global strain level of 1.2%.

## 6 CONCLUSION

A meso-scale finite element based methodology was introduced and applied to study the progressive damage behaviour of triaxially braided composite. We propose that a predictive model should be able to capture both the global stress-strain behaviour and progressive damage process during the loading period. Based on this concept, we identified that the definition of boundary conditions affects significantly the mechanical performance of the model. And to correlate with experiments, the model should be representative in the following two aspects: sufficient number of unit cells to represent the realistic width of the sample due to the presence of size effect, and applying of periodic boundary condition to represent the geometric continuous. The numerical results elaborate that the developed meso-scale model with periodic boundary condition predicts the free-edge effect under both axial and transverse tension case in a very good manner. While the model with simplified symmetrical boundary condition although is able to match the global stress-strain responses, shows limitations in modeling the inherent damage behavior and failure progression. More specifically, the material shows obvious size dependency of measured mechanical properties, which is identified to be caused by the geometric feature induced tension-torsion coupling at the free-edge zones.

The meso-scale finite element model is also applied to study the axial and transverse response of notched coupon and tube specimens, and evaluate their capabilities in obtaining accurate measured mechanical properties. The presented results elaborate the designing purpose of these two kinds of specimens using the strain contour plots and show good agreement with experimental results. The preliminary results indicate that the complicated geometry and large size of the specimens produce difficulties in the numerical modeling, and limit the evaluation ability of this meso-scale model. Overall, the meso-mechanical model is a good tool for virtual testing of this type of materials. The current work provides insights on approaches of meo-mechanical model and its potential application for virtual testing.

## REFERENCES

- [1] R.K. Goldberg, B.J. Blinzler, W.K. Binienda, Investigation of a macromechanical approach to analyzing triaxially braided polymer composites, *AIAA J*, **49**, 2011, pp. 205–215.
- [2] D.S. Ivanov, F. Baudry, B.V. Broucke, S.V. Lomov, H. Xie, I. Verpost, Failure analysis of triaxial braided composite, *Composites Science and Technology*, **69**, 2009, pp. 1372–1380.
- [3] J.A. Schultz, M.R. Garnich, Meso-scale and multicontinuum modeling of a triaxial braided textile composite, *Journal of Composite Materials*, **47**, 2013, pp. 303–314.

- [4] S.V. Lomov, D.S. Ivanov, I. Verpoest, M. Zako, T. Kurashiki, H. Nakai, Meso-FE modelling of textile composites: road map, data flow and algorithms, *Composites Science and Technology*, 67, 2009, pp. 1870–91.
- [5] C. Zhang, W.K. Binienda, A meso-scale finite element model for simulating free-edge effect in carbon/epoxy textile composite, *Mechanics of Materials*, 76, 2014, pp. 1–19.
- [6] C. Zhang, W.K. Binienda, L.W. Kohlman, R.K. Goldberg, Meso-scale failure modeling of single layer triaxially braided composite using finite element method, *Composites Part A*, 58, 2013, pp. 36–46.
- [7] C. Zhang, W.K. Binienda, L.W. Kohlman, Analytical model and numerical analysis of the elastic behavior of triaxial braided composites, *Journal of Aerospace Engineering*, 27, 2013, pp. 473–83.
- [8] C. Zhang, W.K. Binienda, R.K. Goldberg, Free-edge effect on the effective stiffness of single-layer triaxially braided composite, *Composites Science and Technology*, 107, 2015, pp. 145-153.
- [9] J.D. Littell, The experimental and analytical characterization of the macromechanical response for triaxial braided composite, Doctor Dissertation, Department of Civil Engineering, The University of Akron, Akron, 2008.
- [10] C. Zhang, N. Li, W. Wang, W.K. Binienda, H. Fang, Progressive damage simulation of triaxially braided composite using a 3d meso-scale finite element model, *Composite Structures*, 125, 2015, pp. 104-116.
- [11] L.W. Kohlman, Evaluation of test methods for triaxial braided composites and the development of a large multiaxial test frame for validation using braided tube specimens, Doctor Dissertation, Department of Civil Engineering, The University of Akron, Akron, 2010.
- [12] S. Song, A.M. Waas, K.W. Shahwan, O. Faruque, X. Xiao, Compression response, strength and post-peak response of an axial fiber reinforced tow, *International Journal of Mechanical Science*, 51, 2009, pp. 491–9.
- [13] X. Li, W.K. Binienda, R.K. Goldberg, Finite-element model for failure study of two-dimensional triaxially braided composite, *Journal of Aerospace Engineering*, 24, 2010, pp. 170–80.
- [14] S.C. Quek, A.M. Waas, K.W. Shahwan, V. Agaram, Compressive response and failure of braided textile composites: Part 2 – Computations, *International Journal of Non-Linear Mechanics*, 39, 2004, pp. 649–63.
- [15] A.B.H. Kueh, Size-influenced mechanical isotropy of singly-ply triaxially woven fabric composites, *Composites Part A*, 57, 2013, pp.76-87.